

## ORIGINAL ARTICLE

## DNA hypomethylation of inflammation-associated genes in adipose tissue of female mice after multigenerational high fat diet feeding

Y Ding<sup>1,2,6</sup>, J Li<sup>1,2,6</sup>, S Liu<sup>1</sup>, L Zhang<sup>1</sup>, H Xiao<sup>1</sup>, J Li<sup>1</sup>, H Chen<sup>3</sup>, RB Petersen<sup>4</sup>, K Huang<sup>3,5</sup> and L Zheng<sup>1,2</sup>

**OBJECTIVE:** Maternal obesity significantly increases the susceptibility of offspring to develop obesity and chronic diseases in adulthood. The offspring of obese mothers are shown to prefer high fat diet (HFD) due to their altered neural circuitry, creating a 'feed-forward cycle' across generations. We hypothesized that the 'feed-forward cycle' caused by multigenerational HFD feeding would have exacerbated effects in adipose tissue of the offspring.

**METHODS:** Three generations (F0, F1 and F2) of HFD (60% Kcal fat)-fed and corresponding normal chow (NC)-fed C57BL/6 mice were generated. Body weight (BW) and food intake were monitored weekly. Parametrial adipose tissue (pAT) weight and endocrine parameters were measured in 9-month-old female offspring. Gene expression microarray, quantitative RT-PCR and bisulfite sequencing were performed using pAT.

**RESULTS:** BW and pAT weight increased in female mice across generations under continuous HFD stress, with the most severe phenotype found in the F2 generation. Genes involved in inflammatory response showed increased expression across generations in the pAT, accompanied by increased macrophage infiltration. The promoters of Toll-like receptor 1 (*Tlr1*), *Tlr2* and linker for activation of T cells (*Lat*) were hypomethylated in the HF groups compared with the NC group, with additional hypomethylation on some specific CpG sites in the F2 generation.

**CONCLUSIONS:** A feed-forward cycle exists in female mice after continuous HFD stress as demonstrated by increased adiposity and progressive inflammation in adipose tissue across generations. DNA hypomethylation over generations lead to epigenetically altered expression of *Tlr1*, *Tlr2* and *Lat*, which may contribute to the inflammation in adipose tissue. Our study provides a potential mechanism for enhanced inflammation in adipose tissue under multigenerational HFD-fed stress.

*International Journal of Obesity* (2014) 38, 198–204; doi:10.1038/ijo.2013.98

**Keywords:** mouse model; high fat diet; feed-forward cycle; adipose tissue; inflammation; DNA hypomethylation

## INTRODUCTION

One-third of the world's adult population was overweight or obese in 2005, and it is estimated that half of the world's adult population will be overweight or obese by 2030.<sup>1</sup> As a consequence, the economic burden of obesity is rising dramatically, mostly due to obesity-related chronic diseases, including diabetes, cardiovascular disease and cancer.<sup>2</sup>

Furthermore, the onset of obesity is occurring at much younger ages in the past decade than in previous generations.<sup>2</sup> This disproportionate early onset of obesity can be partially explained by Baker's 'fetal origins of adult disease' hypothesis,<sup>3</sup> which is supported by the fact that high fat diet (HFD) intake during pregnancy and lactation increases the rates of obesity and metabolic disorders in the offspring.<sup>4</sup> Moreover, the offspring of obese mothers are shown to prefer HFD due to their altered neural circuitry,<sup>5,6</sup> which generates the next generation of obese mothers and the corresponding obese grand-offspring. This multigenerational HFD-driven obesity is regarded as a

'feed-forward cycle', which may be responsible for the global pandemic of overweight and obesity over the past three decades.

Studies have suggested that a 'feed-forward cycle' exists in rodents, as continuously feeding animals with HFD results in increased body weight (BW) and exacerbated metabolic syndromes over generations.<sup>7–9</sup> However, the exact mechanism(s) underlying these exacerbated phenotypes over generations remain unclear.

In the present study, continuous HFD-fed stress was set up in C57BL/6 mice as previously reported.<sup>7</sup> The multigenerational impacts on adipose tissue after continuous HFD feeding were studied in the female offspring, as the accumulation of white fat weight over generations was observed in the females but not in the males. Genome-wide screening for multigenerational effects of HFD on gene expression was performed and verified. The changes in DNA methylation on the promoters of some genes whose expression was altered over generations were investigated. We found that continuous over-nutrition for three generations

<sup>1</sup>College of Life Sciences, Wuhan University, Wuhan, People's Republic of China; <sup>2</sup>Diabetes Center, Wuhan University, Wuhan, People's Republic of China; <sup>3</sup>Tongji School of Pharmacy, Huazhong University of Science and Technology, Wuhan, People's Republic of China; <sup>4</sup>Departments of Pathology, Neuroscience and Neurology, Case Western Reserve University, Cleveland, OH, USA and <sup>5</sup>Centre for Biomedicine Research, Wuhan Institute of Biotechnology, Wuhan, People's Republic of China. Correspondence: Dr K Huang, Tongji School of Pharmacy, Huazhong University of Science and Technology, Wuhan 430030, China or Dr L Zheng, College of Life Sciences, Wuhan University, Luojia Hill, Wuhan 430072, China.

E-mail: kunhuang2008@hotmail.com or lzheng217@hotmail.com

<sup>6</sup>These authors contributed equally to this work.

Received 27 November 2012; revised 1 March 2013; accepted 4 April 2013; accepted article preview online 27 May 2013; advance online publication, 18 June 2013

resulted in enhanced inflammatory gene expression and macrophage infiltration in adipose tissue through accumulated DNA hypomethylation in the promoters of these genes over multiple generations, especially in the grand-offspring. Our study provides a potential epigenetic mechanism for the epidemic of obesity, which indicates that without urgent and effective intervention, this situation may get worse in successive generations.

## METHODS

### Mice and animal care

C57BL/6 breeding pairs were obtained from the Wuhan University Animal Laboratory and fed with normal chow (NC) to generate the F0 generation for the present study. The female mice of the F0 generation were fed either NC or HFD (60% Kcal fat, D12492, Research Diets Inc, New Brunswick, NJ, USA) for 1 month after weaning and then randomly mated with males fed with NC to generate NC/HF F1 generation. After weaning, female offspring of NC-fed or HFD-fed mothers were continuously fed with NC or HFD, respectively. Two-month-old F1 females were randomly mated with NC-fed males to generate NC/HF F2 generation (A schematic chart of experimental design is provided in Supplementary Figure S1). BW and food intake were monitored weekly except during the mating, pregnancy and lactation periods. In all, 4–8 litters were obtained from each female in the present study. All mice used in the present study were under five generations from the original stock mice. All animals were housed in ventilated microisolator cages with 12 h/12 h light/dark cycle and free access to water according to the Guidelines of the China Animal Welfare Legislation, as approved by the Committee on Ethics in the Care and Use of Laboratory Animals of College of Life Sciences, Wuhan University, Wuhan, People's Republic of China. Nine-month-old female offspring were killed and the organs were dissected and weighted. Visceral parametrial adipose tissue (pAT) was used in the present study, because the visceral fat pads have been shown to have stronger correlation with metabolic diseases than subcutaneous fat pads.<sup>10,11</sup> The gonadal fat pad is easy to locate and is consequently the most studied fat pad. The right side of pATs were stored at  $-80^{\circ}\text{C}$  until use, and the left side of pATs were fixed for histological study.

### Serum levels of insulin and leptin

Serum samples were collected for insulin and leptin analysis. Measurements were performed using an insulin ELISA Kit (Millipore Corporation, Billerica, MA, USA) and a leptin ELISA Kit (Millipore Corporation) according to the manufacturers' instructions.

### Adipocyte size analysis

pAT was fixed with HISTOCHOICE TISSUE FIXATIVE (Amresco, Solon, OH, USA), embedded in paraffin, sectioned and stained with Periodic acid-Schiff. High-resolution ( $\times 200$  magnification) pictures of six different areas from 1–2 sections per sample were taken using an Olympus BX60 microscope equipped with a digital CCD (Olympus Corporation, Tokyo, Japan). Total areas of adipocytes were traced manually and analyzed with Image-Pro Plus 6.0 (Media Cybernetics, Silver Spring, MD, USA) as previously described.<sup>12</sup> For each sample, 400–1000 adipocytes were counted.

### Immunohistochemical study

Fat sections were deparaffinized and rehydrated in decreasing concentrations of ethanol. Sections were incubated with 3%  $\text{H}_2\text{O}_2$  for 5 min to quench endogenous peroxidase activity.<sup>13</sup> After blocking with 5% bovine serum albumin, sections were incubated with primary antibody against F4/80 (1:200 dilution; Santa Cruz Biotechnology, Santa Cruz, CA, USA) overnight at  $4^{\circ}\text{C}$ . After extensive washing, sections were incubated with biotinylated anti-rat immunoglobulin G (Zhongshan Goldenbridge Biotechnology Co., Beijing, China) for 1 h at room temperature. Staining was visualized by DAB (3,3'-diaminobenzidine) substrate (Vector laboratories, Burlingame, CA, USA) following the ABC kit (Vector laboratories). Slides were counterstained with hematoxylin (Beyotime Institute of Biotechnology, Shanghai, China). Negative controls were set up in parallel without applying primary antibody. For each individual adipose tissue, 5–10 different high-resolution ( $\times 200$  magnification) fields from 1–2 sections were analyzed. The percentage of macrophages was calculated as the number of nuclei of F4/80<sup>+</sup> cells divided by the total number of nuclei in the section as previously described.<sup>14</sup>

### Quality control and preprocessing of microarray data

Total RNA was extracted from pAT using RNAiso Plus (Takara Biotechnology Co., Dalian, China) according to the manufacturer's instructions and quantified using a NanoDrop 2000 spectrometer (Thermo Scientific Inc., Wilmington, DE, USA). Pooled total RNA samples from each group were obtained by randomly picking and combining an equal amount (1  $\mu\text{g}$  total RNA per sample) at a designated  $n$  number from each group (NC group:  $n=3$ ; HF F0 group:  $n=4$ ; HF F1 group:  $n=4$ ; HF F2 group:  $n=4$ ) and were used for microarray analysis. Pooling RNA samples for microarray has been used to get an appropriate and statistical estimate of the mean changes among the different experimental groups.<sup>15,16</sup> Mouse WG-6 v2.0 Expression BeadChips (catalog no. BD-201-0202, Illumina Inc., San Diego, CA, USA) were used. The raw intensity was scanned and extracted using BeadArray Reader (Illumina), with the data corrected by background subtraction and normalized using GenomeStudio V2010.2 module (Illumina). Individual mRNAs were examined using the detection  $P$ -value metric provided by Illumina in which the signal generated from each mRNA is compared with negative controls. A threshold of  $P<0.05$  was used as a cutoff. The mRNAs that did not reach this threshold were not analyzed further.

### Microarray data analyses for genes altered across generations

The gene expression levels of different HFD-fed groups were normalized to those of the NC group. Genes of interest were identified as the genes' whose ratios were altered greater than 1.5-fold and the detection  $P$ -values were  $<0.05$ . Heat maps were drawn by R (<http://www.R-project.org>),<sup>17</sup> and Gene Ontology term enrichments were analyzed by DAVID (<http://david.abcc.ncifcrf.gov>).<sup>18</sup> Categories enriched in each list as compared with the *Mus musculus* background were identified by the DAVID  $P$ -value, and those DAVID  $P$ -value  $<0.05$  were selected for subsequent analysis. DAVID was also used to determine genes enriched in KEGG (Kyoto Encyclopedia of Genes and Genomes) pathways.

### Quantitative real-time PCR

cDNA of pAT from each sample was generated using the M-MLV First Strand Kit (Invitrogen, Carlsbad, CA, USA; 1  $\mu\text{g}$  total RNA per sample).<sup>19</sup> Transcript-specific primers were designed using Primer 3.0,<sup>20</sup> and the sequences of primers used in the present study are listed in Supplementary Table S5. *Gapdh* (glyceraldehyde 3-phosphate dehydrogenase) was used as the internal control.<sup>21</sup> Quantitative real-time PCRs were run using a CFX96 Touch Real-Time PCR Detection System (Bio-Rad, Hercules, CA, USA). The relative differences were expressed as fold changes of the different HFD-fed groups over NC group using the  $2^{-\Delta\Delta\text{CT}}$  method.<sup>22</sup>

### Bisulfite sequencing

Genomic DNA from pAT was prepared by standard phenol/chloroform extraction and ethanol precipitation. Bisulfite modification of extracted DNA was performed using the EZ DNA Methylation Gold Kit (Zymo Research, Orange, CA, USA) according to the manufacturer's instructions. The promoters ( $-1200$  bp to  $+200$  bp relative to the  $+1$  transcription start site) of linker for activation of T cells (*Lat*), Toll-like receptors (*Tlr1*) and *Tlr2* were amplified using specific primers designed with MethPrimer (Supplementary Table S6).<sup>23</sup> PCRs were performed using ZymoTaq Polymerase (Zymo Research). The PCR fragments were purified from agarose gels and cloned into the pMD18-T vector (Takara Biotechnology Co.). At least 10 clones of each sample were selected and sequenced by the Beijing Genomics Institute (BGI) ([www.genomics.org.cn](http://www.genomics.org.cn)).

### Statistical analysis

Differences between the groups were analyzed using an analysis of variance *post hoc* test. Statistical significance was defined as  $P\leq 0.05$ , and changes were considered to be trends when  $0.05 < P < 0.07$ .

### Accession numbers

All microarray data used in this study have been deposited to the Gene Expression Omnibus web site (<http://www.ncbi.nlm.nih.gov/geo>; accession no. GSE37238).

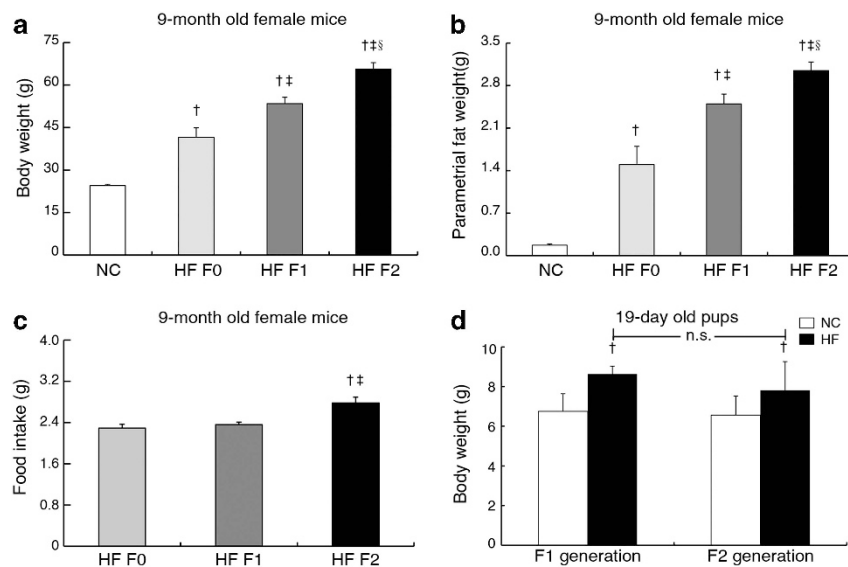


**Figure 1.** Physiological characteristics of the three HFD groups compared with the NC group. **(a)** BW of the four groups. **(b)** Average parametrial fat weight of the four groups. **(c)** Food intake per day for the different HFD-fed groups (data were obtained from 30–36-week-old animals). **(d)** BW of 19-day-old female offspring of F1 and F2 generation fed with NC or HFD. Data are expressed as means  $\pm$  s.d.  $n = 5 \sim 14$  per group. <sup>†</sup> $P < 0.05$  compared with the NC mice; <sup>‡</sup> $P < 0.05$  compared with the HF F0 mice; <sup>§</sup> $P < 0.05$  compared with the HF F1 mice.

## RESULTS

### Physiological characteristics of different experimental groups

As there was no significant difference observed among the NC-fed F0, F1 and F2 females in their basic physiological characteristics (Supplementary Table S1), the three NC-fed female groups were combined into one NC group. BW, pAT weight and body mass index (BMI) were gradually increased in the female offspring across generations under continuous HFD stress, with the heaviest BW, pAT weight and the largest BMI found in the HF F2 group at 9 months of age (Figures 1a and b; Supplementary Table S2). The highest amount of food intake was consistently observed in the HF F2 group (Figure 1c). However, the BWs of 19-day-old female pups were similar between the HF F1 and the HF F2 groups (Figure 1d).

Serum levels of insulin and leptin in the HF groups were elevated compared with the NC group, and these levels were further significantly increased in the HF F1 and HF F2 groups compared with the HF F0 group (Figures 2a and b), indicating much more severe insulin and leptin resistance in the HF F1 and HF F2 groups compared with the HF F0 group at 9 months of age. However, there was no difference in the non-fasted blood glucose levels among the three HFD-fed groups (Supplementary Table S2).

### Morphological changes in the white adipose tissue over generations under continuous HFD stress

Compared with the NC group, the average adipocyte size of the HF F0, HF F1 and HF F2 groups was increased by 5.0-, 4.6- and 4.3-fold, respectively, in 9-month-old females (Figures 3a and b). An unexpected mild, but significant, decrease in the average adipocyte size was observed in the HF F2 group compared with the HF F0 group (Figures 3a and b) due to a significant increase in the population of small-size adipocytes (area  $< 2500 \mu\text{m}^2$ ) and a significant decrease in the population of large-size adipocytes (area  $> 4900 \mu\text{m}^2$ ) in the HF F2 group compared with the HF F0 group (Figures 3c and d).

Infiltrating macrophages, which formed crown-like structures around dead adipocytes, are the major histological feature of inflamed adipose tissue.<sup>24</sup> Immunohistochemistry of F4/80, a well-known macrophage marker,<sup>25</sup> was performed to investigate macrophage infiltration in the sections of adipose tissue. Crown-like structures appeared with greater frequency in the HF F0 and

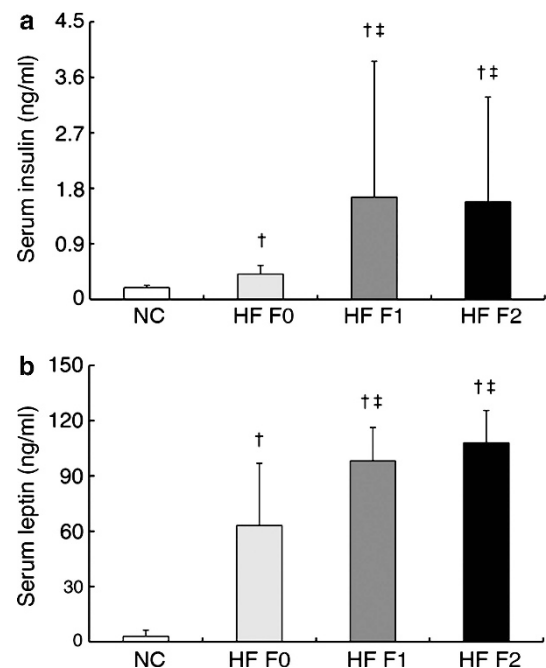


**Figure 2.** Serum insulin **(a)** and leptin **(b)** levels of the four groups. Data are expressed as means  $\pm$  s.d.  $n = 5 \sim 14$  per group. <sup>†</sup> $P < 0.05$  compared with the NC mice; <sup>‡</sup> $P < 0.05$  compared with the HF F0 mice.

HF F1 groups compared with the NC group, with a further increase in the HF F2 group compared with the HF F0 and the HF F1 groups at 9 months of age (Figure 4a). The number of macrophages in the HF F0, HF F1 and HF F2 groups was elevated by 5.5-, 5.7- and 9.5-fold, respectively, compared with the NC group (Figure 4b).

### Alteration of gene transcripts in the white adipose tissue over generations under continuous HFD stress

Genome-wide microarray was performed. When the data were analyzed with the threshold set at a 1.5-fold change, 270 genes

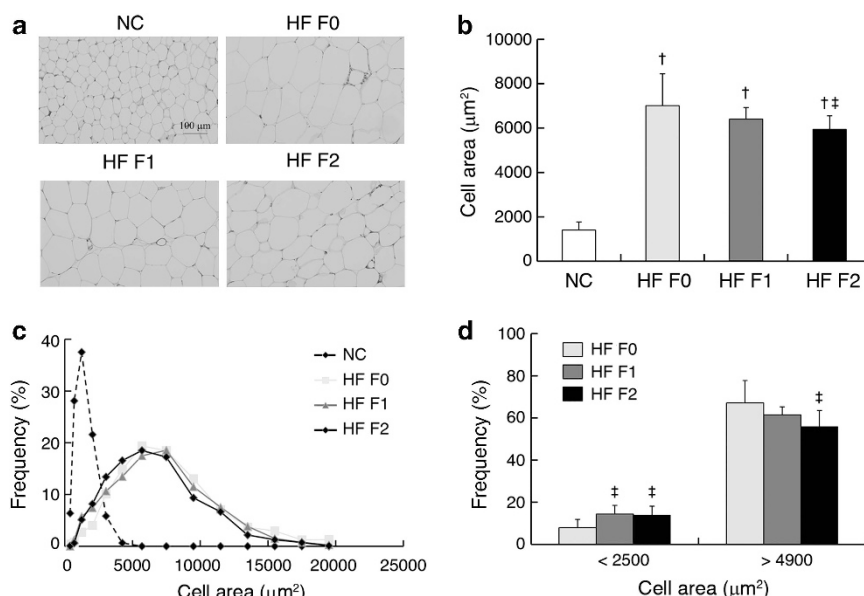


**Figure 3.** Characteristics of the parametrial white adipose tissue of the three HFD groups compared with the NC group. (a) Periodic acid-Schiff (PAS)-stained adipocyte of the four groups. (b) Average adipocyte size of the four groups. (c, d) Adipocyte size distribution analysis of the four groups.  $n = 4 \sim 5$  per group. Data are expressed as means  $\pm$  s.e.m. <sup>†</sup> $P < 0.05$  compared with the NC mice; <sup>‡</sup> $P < 0.05$  compared with the HF F0 mice.

were identified that consistently changed over the generations, among which 183 genes were upregulated and 87 genes were downregulated (Figure 5a). Using Gene Ontology enrichment analysis, some interesting categories were enriched over generations, including response to external stimulus ( $P < 3.7 \times 10^{-9}$ ), high-density lipoprotein particle ( $P < 7.5 \times 10^{-6}$ ), immune system process ( $P < 1.1 \times 10^{-5}$ ), leukocyte activation ( $P < 1.8 \times 10^{-5}$ ) and inflammatory response ( $P < 2.2 \times 10^{-5}$ ) (Supplementary Table S3). KEGG pathway analysis of the genes altered over generations revealed the involvement of peroxisome proliferator-activated receptor signaling pathway, type 2 diabetes mellitus, B-cell and T-cell receptor signaling pathways, TLR signaling pathway and cytokine-cytokine receptor interaction (Supplementary Table S4).

The levels of some genes whose expression was altered over generations were further verified by quantitative real-time PCR (Figures 5b–e). Besides the well-known inflammatory genes, inhibitor of kappaB kinase beta (*Ikkbb*) and tumor necrosis factor (*Tnf*), the levels of NLR family, CARD domain containing 4 (*Nlr4*) and serine (or cysteine) peptidase inhibitor, clade A, member 1A (*Serpina1a*) were also found to be gradually upregulated over generations (Figure 5b). Moreover, a drastic elevation of *Lat*, which has a critical role in T-cell activation,<sup>26</sup> was observed in the HF F2 group (Figure 5b). Interestingly, the mRNA levels of TLRs, such as *Tlr1*, *Tlr2*, *Tlr4*, *Tlr7* and *Tlr8* were also elevated over generations (Figure 5c). In addition, the mRNA levels of apolipoprotein families, including apolipoprotein A-I (*Apoa1*), apolipoprotein A-II (*Apoa2*) and apolipoprotein C-IV (*ApoC4*), were elevated over generations (Figure 5d). Moreover, decreases in the mRNA levels of uncoupling protein 1 (*Ucp1*) and cytosolic phosphoenolpyruvate carboxykinase (*Pck1*) over generations were observed (Figure 5e).

In addition, using *Tlr1* and *Tlr2* as examples, the mRNA levels of these two genes were not significantly changed between the NC F1 and the NC F2 groups (Supplementary Figure S2), which indicated that the transcriptional levels of inflammatory genes are relatively stable over generations under NC feeding.

Decreased DNA methylation in inflammatory genes over generations under continuous HFD stress

DNA methylation is one of the key mechanisms that regulate gene transcription and is also a stable epigenetic marker<sup>17</sup> that we

hypothesize may be responsible for the observed changes in gene expression after multigenerational HFD-fed stress. Bisulfite sequencing was performed to determine the methylation status of the promoters of *Tlr1*, *Tlr2* and *Lat* (Figures 6a–c). Remarkably, the promoters of *Tlr1* and *Tlr2* not only showed significant hypomethylation in the HF F2 group compared with the NC group but also showed a significant hypomethylation on specific CpG sites compared with the HF F0 group or the HF F1 group (Figures 6a and b). In addition, specific CpG sites on the promoter of *Lat* also showed significant hypomethylation in the HF F2 group compared with the NC group (Figure 6c). Moreover, using *Tlr2* and *Lat* as examples, DNA methylation status was not altered between the NC F0 and the NC F2 groups (Supplementary Figure S3), which confirmed that the alterations in DNA methylation status were caused by continuous HFD feeding stress.

The mRNA levels of DNA methyltransferases were also investigated. DNA methyltransferase 1 (*Dnmt1*) was upregulated in the HF F0 and the HF F1 groups compared with the NC group, with a further increase in the HF F2 group compared with the HF F0 and HF F1 groups (Figure 6d). *Dnmt3a* showed a trend toward increase in all the three HFD groups compared with the NC group, while the mRNA levels of *Dnmt3b* was similar among all the experimental groups (Figure 6d).

## DISCUSSION

Maternal obesity is a well-known risk factor that significantly increases the susceptibility of offspring to develop obesity and other chronic metabolic diseases.<sup>4</sup> As food is readily available in many countries these days, and obese mothers are likely to offer more food to their children,<sup>27</sup> humanity is facing continuous over-nutrition stress worldwide. We demonstrated in the present study and in our previous study<sup>7</sup> that continuous HFD feeding stress on mothers show accumulated effects to their offspring, which suggests that, in the future, humanity may face not only an alarming prevalence of obesity but also increased severity of metabolic diseases.

As the BW and pAT weight of 9-month-old female offspring were gradually increased over generations under continuous HFD stress with the most severe phenotype found in the F2 generation



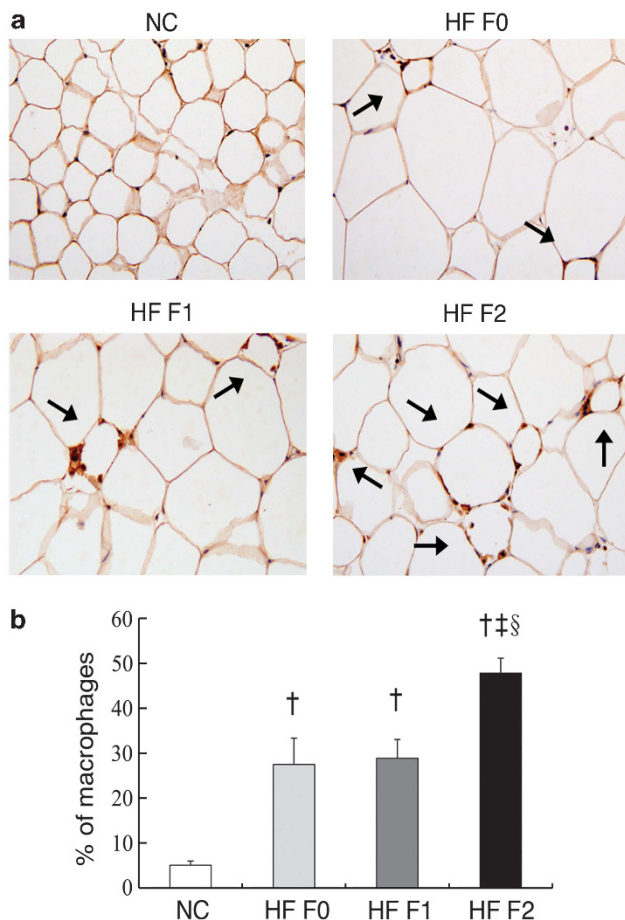


**Figure 4.** Infiltrating macrophages in adipose tissue of the four different groups. **(a)** Adipose tissue F4/80 staining of female offspring from 30–36 weeks of age in the four different experimental groups. **(b)** Macrophages as a percentage of all cells in pAT.  $n = 4 \sim 5$  per group. Data are expressed as means  $\pm$  s.e.m. † $P < 0.05$  compared with the NC mice; ‡ $P < 0.05$  compared with the HF F0 mice; § $P < 0.05$  compared with the HF F1 mice.

(grand-offspring; Figures 1a and b), and the BWs of 19-day-old female pups are similar between the HF F1 and HF F2 groups (Figure 1d), the accumulation of adiposity we found in this study is likely not simply due to developmental over-nutrition (during pregnancy and lactation stages) but also reflects over-nutrition in the adult stage.

In the present study and our previous study,<sup>7</sup> we found that both male and female offspring showed increased BW and BMI over generations under multigenerational HFD feeding stress. Sexual dimorphism in weight accumulation of different organs was also observed. Increased liver weight, but not the weight of white adipose tissue, was previously demonstrated by us in the male offspring under multigenerational HFD feeding stress.<sup>7</sup> Under the same stress, the weight of white adipose tissue, but not the liver, was increased over generations in the female offspring (Figure 1b and Supplementary Table S2). Consistent with our data, the weight of white adipose tissue was also increased over generations in the ICR females, but not in the males, under multigenerational over-nutrition.<sup>8</sup> Compared with female mice, male mice are usually more susceptible to diet-induced obesity in the F0 generation at young ages.<sup>28,29</sup> However, a recent study using C57BL/6N mice demonstrated that although males have heavier weights than females before 20 weeks when they are fed the obesity-promoting HFD, females and males show comparable weights at 35 weeks, with more severe fat accumulation and larger adipocytes found in females.<sup>30</sup> Furthermore, the maternal

obesity models suggested the female offspring are preferentially affected by maternal diets.<sup>31,32</sup> Sex hormone may be one of the players that contribute to this interesting phenomenon; however, the exact mechanism under this multigenerational over-nutrition feeding stress-induced sexual dimorphism requires further investigation.

The contribution of inflammation to obesity-associated insulin resistance has been well documented.<sup>33</sup> The major cluster of upregulated genes caused by multigenerational HFD feeding stress in female mice is related to inflammation (Figures 5a–c; Supplementary Tables S3 and S4), with the histological demonstration of elevated infiltrating macrophages over generations (Figures 4a and b). These infiltrated macrophages have been reported to release a variety of proinflammatory cytokines, which cause decreased insulin sensitivity.<sup>33</sup> Interestingly, we also noticed the multigenerational elevation of *Nlr4* and *Tlr5*, both of which are innate immune receptors sensing pathogen-associated molecular patterns.<sup>34</sup> *Nlr4* is a critical component in the formation of the inflammasome, which has been demonstrated to have important roles in inflammation and insulin sensitivity.<sup>35</sup> Knockout of *Tlr2* or *Tlr4* has been shown to protect mice against HFD-induced inflammation in adipose tissue.<sup>36,37</sup> Furthermore, *Tlr4* has a critical role in the inhibition of *Pck1* expression in adipose tissue after multiple inflammatory injuries.<sup>38</sup> Consistent with this report, the mRNA levels of *Pck1* were found to be downregulated over generations in the present study (Figure 5e). Future study is needed to investigate whether downregulation of *Tlr5* or *Nlr4* can disrupt the 'feed-forward cycle'.

In the adipose tissue, white adipocytes and brown adipocytes are intermingled and can transdifferentiate with each other.<sup>39</sup> The white adipocyte has a large unilocular lipid droplet, which serves as an energy storage place.<sup>40</sup> The brown adipocyte has multilocular lipid droplets and large mitochondria.<sup>40</sup> UCP1 is a protein expressed in the internal membrane of brown adipocyte mitochondria and is responsible for heat production.<sup>41</sup> The mRNA levels of *Ucp1* in the interscapular brown fat are four magnitudes higher than that found in the pAT (unpublished data by Yingwen Ding and Ling Zheng). The downregulation of *Ucp1* found in the present study (Figure 5e) may indicate that the adipose tissue gradually lost the 'brown' characteristics over generations.

Epigenetic regulation, including DNA methylation and histone modification, has provided new insights into the multigenerational inheritance of disease risk.<sup>42</sup> Previously, studies indicated that maternal obesity induces alterations of metabolic genes in the F1 generation by epigenetic modifications.<sup>5,43,44</sup> We also found multigenerational alteration of histone methylation in the livers of male offspring after three generations of over-nutrition.<sup>7</sup> Compared with the complex and dynamic changes in histone modifications, DNA methylation is the only epigenetic marker on DNA and is regarded as a more stable epigenetic marker.<sup>17</sup> DNA methylation patterns can be transmitted over one generation in the germ line.<sup>45,46</sup> To our knowledge, the present study demonstrates, for the first time, a multigenerational effect on DNA methylation in the offspring through the maternal lineage. The gradual hypomethylation in the promoters of inflammation-related genes (Figures 6a–c) leads to multigenerationally exacerbated inflammation in adipose tissue under continuous HFD feeding stress. We noticed, compared with the changes of the mRNA levels, the alteration in DNA methylation is mild over generations under the continuous HFD feeding stress. As there are multiple methylation sites in the regulatory sequence of a gene, it is possible that these subtle changes in DNA methylation have an additive effect on the final expression level of the gene. Also a larger sample size may be required to detect smaller effect sizes. Furthermore, other epigenetic regulation such as histone modification may also contribute to enhanced inflammation over generations in adipose tissue due to the complex cross-talk between DNA methylation and histone modification.<sup>17</sup> At the

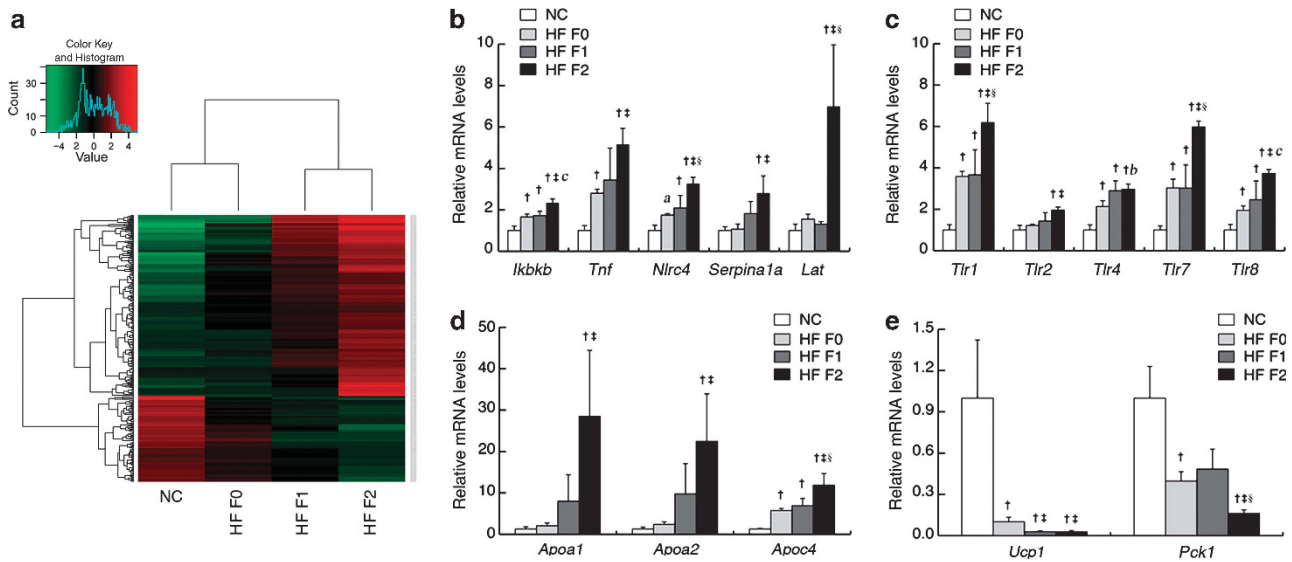


**Figure 5.** Gene expression levels altered over generations in the adipose tissue of the 9-month-old female offspring. (a) Heat map of 270 multigenerational altered genes in adipose tissue. (b) mRNA levels of *Ikbkb*, *Tnf*, *Nlr4*, *Serpina1a* and *Lat* involved in inflammatory response. (c) mRNA levels of *Tlr1*, *Tlr2*, *Tlr4*, *Tlr7* and *Tlr8* in the TLR family. (d) mRNA levels of *Apoa1*, *Apo2* and *Apoc4* in the apolipoprotein family. (e) mRNA levels of *Ucp1* and *Pck1*.  $n=4\sim7$  per group. Data are expressed as means  $\pm$  s.e.m.  $^{\dagger}P<0.05$  compared with the NC mice;  $^{\ddagger}P<0.05$  compared with the HF F0 mice;  $^{\S}P<0.05$  compared with the HF F1 mice.  $^{0.05<^aP<0.07}$  compared with the NC mice;  $^{0.05<^bP<0.07}$  compared with the HF F0 mice;  $^{0.05<^cP<0.07}$  compared with the HF F1 mice.

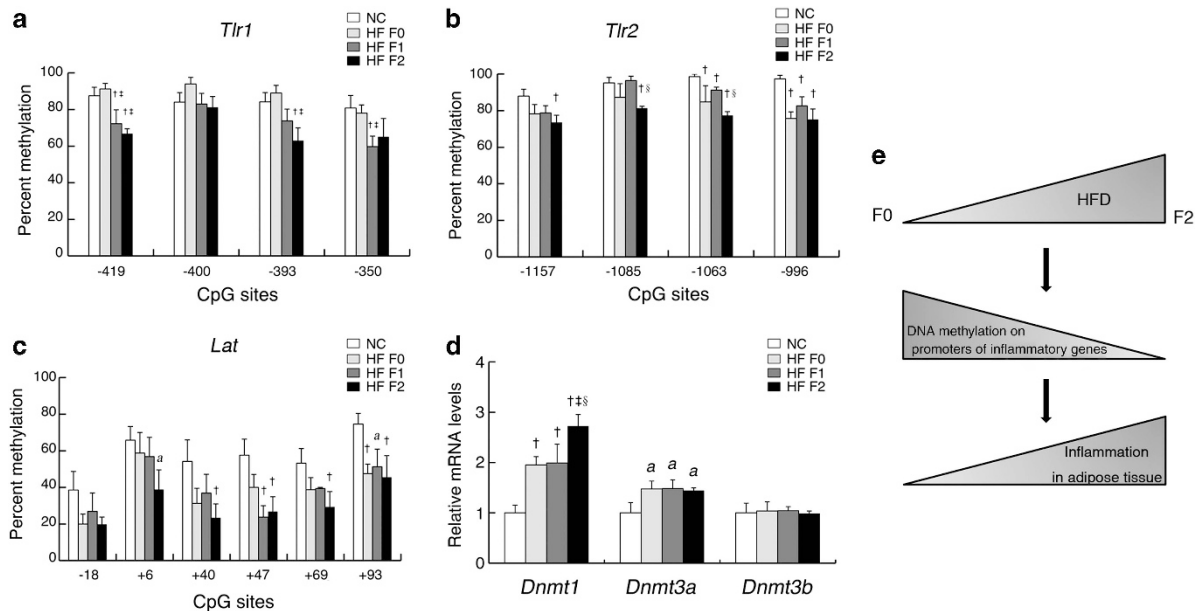


**Figure 6.** Alteration of DNA methylation contributes to the multigenerational changes in gene expression. DNA hypomethylation of *Tlr1* promoter (a), *Tlr2* promoter (b) and *Lat* promoter (c). (d) mRNA levels of *Dnmt1*, *Dnmt3a* and *Dnmt3b* in the adipose tissue of the four groups. (e) Potential mechanisms by which DNA methylation contributes to the 'feed-forward cycle' in adipose tissue.  $n=4\sim5$  per group. Data are expressed as means  $\pm$  s.e.m.  $^{\dagger}P<0.05$  compared with the NC mice;  $^{\ddagger}P<0.05$  compared with the HF F0 mice;  $^{\S}P<0.05$  compared with the HF F1 mice.  $^{0.05<^aP<0.07}$  compared with the NC mice.

same time, we observed a multigenerational elevation of *Dnmt1* in adipose tissue under continuous HFD feeding stress (Figure 6d), which suggests a genome-wide increase in DNA methylation. Similarly, in cancer, DNA methylation status has been observed to be different in the promoters of specific genes compared with the whole genome.<sup>47</sup>

In summary, our data suggested that a feed-forward cycle exists in female offspring after continuous HFD feeding stress as demonstrated by multigenerational increased adiposity and

progressive inflammation in pAT in mice (Figure 6e). Multigenerational changes in DNA hypomethylation on inflammatory genes contribute to the increased inflammation in adipose tissue over generations in mice (Figure 6e). Gonadal white adipose tissue is the most studied fat pad in rodent models; however, it is only exist in rodents. More studies are therefore necessary to investigate the impact of multigenerational HFD stress on fat accumulation in human by public health surveys and other methods. However, the results presented in our study with mice

suggest a potential new mechanism for enhanced inflammation in adipose tissue under continuous HFD stress that may provide new insights on the pandemic obesity in human society.

## CONFLICT OF INTEREST

The authors declare no conflict of interest.

## ACKNOWLEDGEMENTS

We thank Bo Yang (College of Life Sciences, Wuhan University, Wuhan, People's Republic of China) for technical assistance with the heat map and Professor Xin Chen (UCSF, USA) for critical reading the manuscript. This work was supported by the National Basic Research Program of China (2009BC918304 and 2012CB524901), the Natural Science Foundation of China (Nos. 30970607, 81172971, 81222043 and 31271370) and the Program for New Century Excellent Talents in University (NECT10-0623 and NECT11-0170).

## REFERENCES

- Kelly T, Yang W, Chen CS, Reynolds K, He J. Global burden of obesity in 2005 and projections to 2030. *Int J Obes (Lond)* 2008; **32**: 1431–1437.
- Wang YC, McPherson K, Marsh T, Gortmaker SL, Brown M. Health and economic burden of the projected obesity trends in the USA and the UK. *Lancet* 2011; **378**: 815–825.
- Barker DJ. The origins of the developmental origins theory. *J Intern Med* 2007; **261**: 412–417.
- Muhlhauser BS, Ong ZY. The fetal origins of obesity: early origins of altered food intake. *Endocr Metab Immune Disord Drug Targets* 2011; **11**: 189–197.
- Vucetic Z, Kimmel J, Totoki K, Hollenbeck E, Reyes TM. Maternal high-fat diet alters methylation and gene expression of dopamine and opioid-related genes. *Endocrinology* 2010; **151**: 4756–4764.
- Sullivan EL, Smith MS, Grove KL. Perinatal exposure to high-fat diet programs energy balance, metabolism and behavior in adulthood. *Neuroendocrinology* 2011; **93**: 1–8.
- Li J, Huang J, Li JS, Chen H, Huang K, Zheng L. Accumulation of endoplasmic reticulum stress and lipogenesis in the liver through generational effects of high fat diets. *J Hepatol* 2012; **56**: 900–907.
- Takasaki M, Honma T, Yanaka M, Sato K, Shinohara N, Ito J et al. Continuous intake of a high-fat diet beyond one generation promotes lipid accumulation in liver and white adipose tissue of female mice. *J Nutr Biochem* 2011; **23**: 640–645.
- Massiera F, Barbry P, Guesnet P, Joly A, Luquet S, Moreilhon-Brest C et al. A Western-like fat diet is sufficient to induce a gradual enhancement in fat mass over generations. *J Lipid Res* 2010; **51**: 2352–2361.
- Matsuzawa Y, Shimomura I, Nakamura T, Keno Y, Tokunaga K. Pathophysiology and pathogenesis of visceral fat obesity. *Diabetes Res Clin Pract* 1994; **24**(Suppl): S111–S116.
- Hamdy O, Porramatikul S, Al-Ozairi E. Metabolic obesity: the paradox between visceral and subcutaneous fat. *Curr Diabetes Rev* 2006; **2**: 367–373.
- Chen HC, Farese Jr RV. Determination of adipocyte size by computer image analysis. *J Lipid Res* 2002; **43**: 986–989.
- Chen H, Zheng C, Zhang X, Li J, Zheng L, Huang K. Apelin alleviates diabetes-associated endoplasmic reticulum stress in the pancreas of Akita mice. *Peptides* 2011; **32**: 1634–1639.
- Kosteli A, Sgaru E, Haemmerle G, Martin JF, Lei J, Zechner R et al. Weight loss and lipolysis promote a dynamic immune response in murine adipose tissue. *J Clin Invest* 2010; **120**: 3466–3479.
- Peng X, Wood CL, Blalock EM, Chen KC, Landfield PW, Stromberg AJ. Statistical implications of pooling RNA samples for microarray experiments. *BMC Bioinformatics* 2003; **4**: 26.
- Bruce KD, Cagampang FR, Argenton M, Zhang J, Ethirajan PL, Burdge GC et al. Maternal high-fat feeding primes steatohepatitis in adult mice offspring, involving mitochondrial dysfunction and altered lipogenesis gene expression. *Hepatology* 2009; **50**: 1796–1808.
- Cedar H, Bergman Y, Linking DNA. Methylation and histone modification: patterns and paradigms. *Nat Rev Genet* 2009; **10**: 295–304.
- Huang da W, Sherman BT, Lempicki RA. Systematic and integrative analysis of large gene lists using DAVID bioinformatics resources. *Nat Protoc* 2009; **4**: 44–57.
- Wang LL, Chen H, Huang K, Zheng L. Elevated histone acetylations in Muller cell contribute to inflammation: a novel inhibitory effect of minocycline. *Glia* 2012; **60**: 1896–1905.
- Rozen S, Skaletsky H. Primer3 on the WWW for general users and for biologist programmers. *Methods Mol Biol* 2000; **132**: 365–386.
- Barber RD, Harmer DW, Coleman RA, Clark BJ. GAPDH as a housekeeping gene: analysis of GAPDH mRNA expression in a panel of 72 human tissues. *Physiol Genomics* 2005; **21**: 389–395.
- Schmittgen TD, Livak KJ. Analyzing real-time PCR data by the comparative (C<sub>T</sub>) method. *Nat Protoc* 2008; **3**: 1101–1108.
- Li LC, Dahiya R. MethPrimer: designing primers for methylation PCRs. *Bioinformatics* 2002; **18**: 1427–1431.
- Murano I, Barbatelli G, Parisani V, Latini C, Muzzonigro G, Castellucci M et al. Dead adipocytes, detected as crown-like structures, are prevalent in visceral fat depots of genetically obese mice. *J Lipid Res* 2008; **49**: 1562–1568.
- Gordon S, Hamann J, Lin HH, Stacey M. F4/80 and the related adhesion-GPCRs. *Eur J Immunol* 2011; **41**: 2472–2476.
- Balagopalan L, Ashwell BA, Bernot KM, Akpan IO, Quasba N, Barr VA et al. Enhanced T-cell signaling in cells bearing linker for activation of T-cell (LAT) molecules resistant to ubiquitylation. *Proc Natl Acad Sci USA* 2011; **108**: 2885–2890.
- Wardle J, Sanderson S, Guthrie CA, Rapoport L, Plomin R. Parental feeding style and the inter-generational transmission of obesity risk. *Obes Res* 2002; **10**: 453–462.
- Hong J, Stubbins RE, Smith RR, Harvey AE, Nunez NP. Differential susceptibility to obesity between male, female and ovariectomized female mice. *Nutr J* 2009; **8**: 11.
- Stubbins RE, Najjar K, Holcomb VB, Hong J, Nunez NP. Oestrogen alters adipocyte biology and protects female mice from adipocyte inflammation and insulin resistance. *Diabetes Obes Metab* 2012; **14**: 58–66.
- Medrikova D, Jilkova ZM, Bardova K, Janovska P, Rossmelisl M, Kopecky J. Sex differences during the course of diet-induced obesity in mice: adipose tissue expandability and glycemic control. *Int J Obes (Lond)* 2012; **36**: 262–272.
- Bayol SA, Simbi BH, Bertrand JA, Stickland NC. Offspring from mothers fed a 'junk food' diet in pregnancy and lactation exhibit exacerbated adiposity that is more pronounced in females. *J Physiol* 2008; **586**: 3219–3230.
- Khan IY, Taylor PD, Dekou V, Seed PT, Lakasing L, Graham D et al. Gender-linked hypertension in offspring of lard-fed pregnant rats. *Hypertension* 2003; **41**: 168–175.
- Olefsky JM, Glass CK. Macrophages, inflammation, and insulin resistance. *Annu Rev Physiol* 2010; **72**: 219–246.
- Franchi L, Eigenbrod T, Munoz-Planillo R, Nunez G. The inflammasome: a caspase-1-activation platform that regulates immune responses and disease pathogenesis. *Nat Immunol* 2009; **10**: 241–247.
- Vandanmagsar B, Youm YH, Ravussin A, Galgani JE, Stadler K, Mynatt RL et al. The NLRP3 inflammasome instigates obesity-induced inflammation and insulin resistance. *Nat Med* 2011; **17**: 179–188.
- Kuo LH, Tsai PJ, Jiang MJ, Chuang YL, Yu L, Lai KT et al. Toll-like receptor 2 deficiency improves insulin sensitivity and hepatic insulin signalling in the mouse. *Diabetologia* 2011; **54**: 168–179.
- Shi H, Kokoieva MV, Inouye K, Tzamelis I, Yin H, Flier JS. TLR4 links innate immunity and fatty acid-induced insulin resistance. *J Clin Invest* 2006; **116**: 3015–3025.
- Feingold KR, Moser A, Shigenaga JK, Grunfeld C. Inflammation inhibits the expression of phosphoenolpyruvate carboxykinase in liver and adipose tissue. *Innate Immun* 2011; **18**: 231–240.
- Cinti S. Transdifferentiation properties of adipocytes in the adipose organ. *Am J Physiol Endocrinol Metab* 2009; **297**: E977–E986.
- Cinti S. The adipose organ. *Prostaglandins Leukot Essent Fatty Acids* 2005; **73**: 9–15.
- Cinti S. The role of brown adipose tissue in human obesity. *Nutr Metab Cardiovasc Dis* 2006; **16**: 569–574.
- Ozanne SE, Constancia M. Mechanisms of disease: the developmental origins of disease and the role of the epigenotype. *Nat Clin Pract Endocrinol Metab* 2007; **3**: 539–546.
- Ng SF, Lin RC, Laybutt DR, Barres R, Owens JA, Morris MJ. Chronic high-fat diet in fathers programs beta-cell dysfunction in female rat offspring. *Nature* 2010; **467**: 963–966.
- Carone BR, Fauquier L, Habib N, Shea JM, Hart CE, Li R et al. Paternally induced transgenerational environmental reprogramming of metabolic gene expression in mammals. *Cell* 2010; **143**: 1084–1096.
- Cropley JE, Suter CM, Beckman KB, Martin DI. Germ-line epigenetic modification of the murine A<sub>vy</sub> allele by nutritional supplementation. *Proc Natl Acad Sci USA* 2006; **103**: 17308–17312.
- Anway MD, Cupp AS, Uzumcu M, Skinner MK. Epigenetic transgenerational actions of endocrine disruptors and male fertility. *Science* 2005; **308**: 1466–1469.
- Sharma S, Kelly TK, Jones PA. Epigenetics in cancer. *Carcinogenesis* 2010; **31**: 27–36.

Supplementary Information accompanies this paper on International Journal of Obesity website (<http://www.nature.com/ijo>)